
CLEVRER-Humans: Describing Physical and Causal Events the Human Way

Jiayuan Mao*
MIT

Xuelin Yang*
Stanford University

Xikun Zhang
Stanford University

Noah D. Goodman
Stanford University

Jiajun Wu
Stanford University

Abstract

Building machines that can reason about physical events and their causal relationships is crucial for flexible interaction with the physical world. However, most existing physical and causal reasoning benchmarks are exclusively based on synthetically generated events and synthetic natural language descriptions of causal relationships. This design brings up two issues. First, there is a lack of diversity in both event types and natural language descriptions; second, causal relationships based on manually-defined heuristics are different from human judgments. To address both shortcomings, we present the CLEVRER-Humans benchmark, a video reasoning dataset for causal judgment of physical events with human labels. We employ two techniques to improve data collection efficiency: first, a novel iterative event cloze task to elicit a new representation of events in videos, which we term Causal Event Graphs (CEGs); second, a data augmentation technique based on neural language generative models. We convert the collected CEGs into questions and answers to be consistent with prior work. Finally, we study a collection of baseline approaches for CLEVRER-Humans question-answering, highlighting the great challenges set forth by our benchmark.

1 Introduction

The ability to reason about physical events and their causal relationships from visual observations lies at the core of human intelligence. It is crucial for humans to holistically understand and flexibly interact with the physical world [1, 2, 3, 4, 5]. Natural language provides a way for humans to express such causal understanding [6], and we can use natural language as a lens to evaluate machine understanding of physical events and causal judgments. This brings us two major advantages. First, compared to bounding boxes and timecodes, language provides a more flexible interface for describing events. Furthermore, it naturally enables the generation of human-interpretable explanations.

We have seen significant progress toward machine reasoning about physical events and causal structures, driven by datasets such as CLEVRER [7] and CATER [8]. These datasets pair videos containing physical object interactions (e.g., collisions) with natural language question-answer pairs. However, there are two important design flaws in existing datasets. First, the categories of physical events are designed manually and identified through heuristic rules over object locations and velocities, significantly restricting the datasets' diversity. For example, the CLEVRER dataset only contains three types of events (object enter, object exit, and collision). Second, the causal relationships of

*indicates equal contribution. Authors ordered alphabetically. Correspondence to: jiayuanm@mit.edu.

Project page: <https://sites.google.com/stanford.edu/clevrer-humans/home>.

Dataset DOI: <https://doi.org/10.5061/dryad.5tb2rbp7c>.

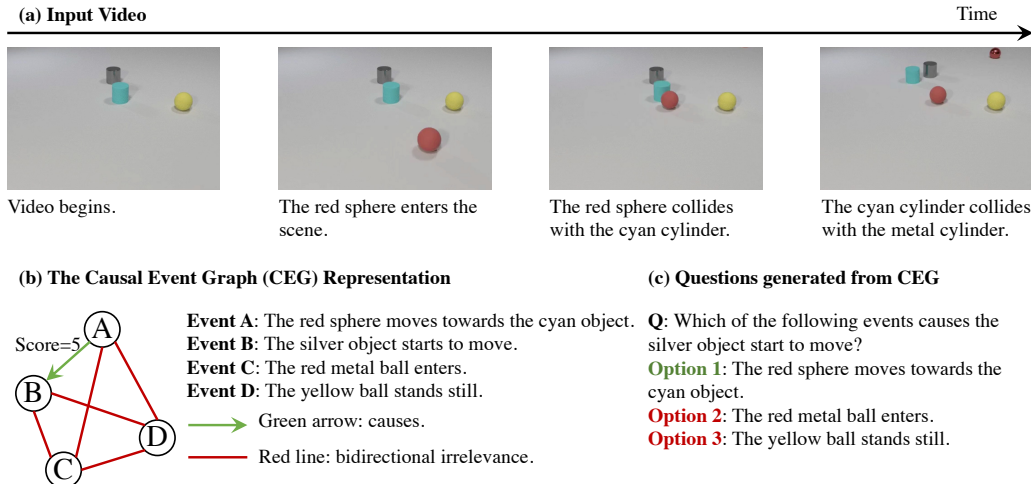


Figure 1: For (a) each video in the CLEVRER dataset, (b) CLEVRER-Humans annotates a human-labeled graphical representation of physical events and their causal relations, in the form of causal event graphs (CEGs). Each CEG composes of a collection of nodes associated with textual descriptions of events, and human-labeled directional edges indicating the causal relationship between objects. Each edge is also associated with a score indicating a human’s graded attribute of causal relations. (c) The compact representation of CEGs can be easily translated into question-answer pairs to evaluate video reasoning models.

events are also detected by heuristic rules. In contrast, human causal judgment resembles complex counterfactual reasoning processes [9, 2, 6], and it is difficult to capture these subtleties through manually specified rules.

To address both shortcomings, we present CLEVRER-Humans, a human-annotated physical and causal reasoning dataset based on videos from CLEVRER [7], of which we show examples in Fig. 1a. To ensure sufficient event diversity and annotation density (i.e., a dense causal relation between events), CLEVRER-Humans relies on a data representation termed Causal Event Graphs [CEG; 7, 10], whose nodes are natural language descriptions of the events in the video and edges are causal relationships between the events, as illustrated in Fig. 1b. The CEG annotation procedure has two stages. In the first stage, we use an iterative event cloze task to collect event descriptions. Specifically, starting from a seeding set of events in the original CLEVRER dataset, we ask annotators to describe other events that are responsible for these seed events. The newly annotated events will be iteratively used as new seeds to progressively grow the annotated events. In the second stage, we condense the CEGs by asking human annotators to make binary classifications of causal influence for all pairs of physical events generated in the first stage. Based on both positive and negative labels, we can construct physical and causal reasoning questions in natural language, shown in Fig. 1c.

One challenge of this pipeline is that human annotation for event cloze tasks is generally time- and budget-consuming. To alleviate this, we leverage the observation that neural generative models are reasonably good at generating event descriptions. Thus, we only collect a small number of physical event descriptions in the first stage. In the second stage, we augment these data by training neural event description models based on the ground truth physical trajectories of objects and ask human annotators to filter incorrect or hard-to-interpret descriptions.

Finally, we benchmark several machine learning models on CLEVRER-Humans. We demonstrate that our dataset is challenging, in particular, due to the diversity of event descriptions and the challenge of data-efficient learning. The development of CLEVRER-Humans can be beneficial to both machine learning and cognitive science communities. From the machine learning perspective, CLEVRER-Humans posits a combined challenge of natural language understanding, physical grounding of language, and causal reasoning in physical scenes. It is also a stimulus set for cognitive science studies of human physical event perception, causal judgment, and description [6, 11].

Dataset	Video	Question Answering	Diagnostic Annotation	Natural Language Events	Causal Reasoning	Human Causal Judgements
CLEVR [12]	-	✓	✓	-	-	-
MovieQA [13]	✓	✓	-	✓	-	-
TGIF-QA [14]	✓	✓	-	✓	-	-
TVQA+ [15]	✓	✓	-	✓	-	-
AGQA [16]	✓	✓	-	✓	-	-
IntPhys [17]	✓	-	✓	-	✓	-
Galileo [18]	✓	-	✓	-	✓	-
PHYRE [19]	✓	-	✓	-	✓	-
CATER [8]	✓	✓	✓	-	✓	-
CoPhy [20]	✓	-	✓	-	✓	-
CRAFT [10]	✓	✓	✓	-	✓	-
CLEVRER [7]	✓	✓	✓	-	✓	-
ComPhy [21]	✓	✓	✓	-	✓	-
CLEVRER-Humans	✓	✓	✓	✓	✓	✓

Table 1: Comparison between CLEVRER-Humans with other visual reasoning benchmarks. Our dataset is the only dataset of natural language descriptions of physical events and human judgments.

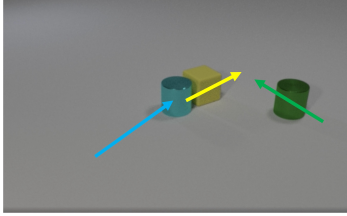
2 Related work

Physical and causal reasoning. Our dataset is closely related to benchmarks on physical reasoning tasks. In general, these benchmarks can be categorized into three groups based on their evaluation protocol. First, datasets such as IntPhys [17], Galileo [18], and CoPhy [20] focus on making counterfactual or hypothetical predictions of physical events. Second, benchmarks including PHYRE [19] and ESPRIT [22] focus on an “inverse” problem of generating initial conditions that leads to a specific goal state. The third group of benchmarks, where our dataset CLEVRER-Humans also falls into, focuses on assessing machine learning models through a natural language interface, such as CATER [8], CLEVRER [7], CRAFT [10], and ComPhy [21]. While these datasets focus on other aspects of physical and causal reasoning, such as physical property inference [18] and few-shot learning [21], their causal relationships and event descriptions are all generated by synthetic rules. By contrast, our dataset contains human-annotated physical event descriptions and causal relationships.

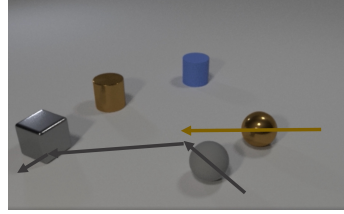
Human causal cognition. Understanding how humans perceive and reason about causal relationships has been a long-standing problem in cognitive science [9]. A number of theories have been proposed to model human causal cognition, such as Force Dynamics [1, 2], Mental Models [23], Causal Models [24, 25], and Counterfactual Simulation [26, 27]. These theories have a variety of aims, including causal induction, causal attribution, and grounding causal language such as "cause", "prevent", "help", "enable", and "allow". In this work, we study the relatively neutral causal connective "because", together with freely-generated descriptions of physical events.

Physical causation, in particular, has received much attention with rich experimental and theoretical literature. Among theories of physical causation judgements: Conserved Quantity Theory [28] predicts causal relations by inspecting how conserved quantities (e.g., momentum) transferred between events. Force Dynamics Theory [FDT; 1, 2] focuses on analyzing the mechanism of causation when bodies interact, using force vectors to represent the interaction between objects, and predicting judgments based on the direction and length of these vectors. Counterfactual Simulation Theory [CSM; 26, 27] leverages an intuitive physics model to make counterfactual judgements (A causes B if A’s occurrence makes a difference to B’s occurrence). These theories often agree on predicted causal judgements, and are very often different from the simple heuristic used to annotate the "responsible for" relation of CLEVRER. There are also critical differences in predictions, particularly for complex events (where it is not always clear how to apply a given theory). Thus it is necessary to collect human judgements of the causal relation between events; in future work, it will be interesting to compare machine learning models derived from our data to psychological theories of physical causation.

Video question answering. The primary task we study is to answer questions about videos of physical scenes. Unlike benchmarks that focus on multi-modal learning in real-world videos about human-



Question: What is responsible for the rubber cube's colliding with the green object?
Choice: The presence of the cyan object.
CLEVRER-Heuristic: Correct
Human: Wrong
Explanation: Humans may think the "presence" is not the direct cause. Instead, the collision between the cyan object is a more direct cause.



Question: What is responsible for the rubber sphere's exiting the scene?
Choice: The presence of the metal sphere.
CLEVRER-Heuristic: Correct
Human: Wrong
Explanation: Even without the presence of metal sphere, the rubber sphere will still exit the scene. Also, before exiting the scene, the rubber sphere collides with the grey cube. Thus, the choice is not the cause.

Figure 2: This are two examples showing difference of human causal judgment and CLEVRER’s heuristic causal relation. The arrows in the image represent the moving direction of objects of interest.

P(X Y)	Y = CLEVRER	Y = Counterfactual	Y = Human
X = CLEVRER	1.00	0.74	0.96
X = Counterfactual	0.89	1.00	0.54
X = Human	0.62	0.61	1.00

Table 2: Comparison between different heuristics-generated causal labels and human labels, on a sampled subset of CLEVRER [7]. The entry $P(X|Y)$ denotes the fraction of event relations that are annotated as causal by protocol X given that the relations are annotated as causal by protocol Y.

human and human-object interactions [13, 14, 15, 16], we focus on understanding physical events and their causal relationships. We summarize the key factors that differentiate our dataset from others in Table 1. Among them, CLEVRER-Humans is the only dataset that contains human-annotated physical events and causal judgements.

Video-conditioned text generation. Our dataset is built on recent advances in using deep neural networks to generate natural language descriptions of videos [29, 30, 31, 32]. A common approach to generating video event descriptions is to first apply per-frame neural network encoders to obtain per-frame features, and aggregate them over time. Popular aggregation algorithms include average pooling [33], recurrent neural networks [34], and attention mechanisms [35]. Our model for event description generation falls into the third group, and leverages temporal attention in generation.

3 CLEVRER-Humans

Our dataset is based on the videos from the CLEVRER dataset [7]. Each video contains at most 5 colliding objects moving on a single plane in 3D. The objects have 3 different shapes (cylinder, cube, and sphere), 8 colors, and 2 materials (rubber and material). The questions in CLEVRER consists of four types: descriptive (“what color”), explanatory (“what’s responsible for”), predictive (“what will happen next”), and counterfactual (“what if”). In this paper, we particularly focus on explanatory questions, which evaluate machine reasoning about causal relationships. Explanatory questions query the causal structure of a video by asking for the cause of an event, providing multiple choices. There are 3 types of events defined in CLEVRER’s explanatory questions: entering the scene, exiting the scene, and colliding with another object. In CLEVRER, the event descriptions are generated by pre-defined templates.

3.1 Delving into Causal Relation Annotations

Before introducing our new dataset CLEVRER-Humans, we start from investigating the divergence between human labels and the labels generated by the original CLEVRER dataset using heuristics. In this section, we will be comparing three labelling protocols on a subset of 50 videos from the CLEVRER dataset. The first method (CLEVRER) uses the heuristic rules defined in the original CLEVRER dataset to predict causal relations between each pair of events. Specifically, if event A

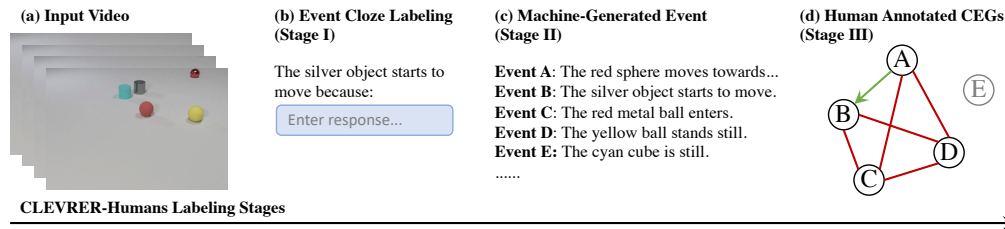


Figure 3: The overall labeling pipeline of CLEVRER-Humans. (a) Starting from input videos, (b) we use an event cloze task to collect a small number of human-written event descriptions about videos (Stage I). (c) Next, we train neural event description generators to augment all videos with a collection of events (Stage II). (d) Finally, human annotators label the correctness of all generated events (in this case, event E is incorrect and thus the node is dropped) as well as their causal relations (Stage III).

happens before event B, and they share at least one object, we say event A is a cause of event B[†]. The second method (Counterfactual) uses counterfactual intervention to derive the causal relationship. Specifically, we say event A causes event B if event A happens before event B and event B happens even if we remove all relevant objects in event A from the scene (except for the objects in event B). We compare these two methods with human labeled causal relations.

We summarize the resulting statistics in Table 2. There is a considerable difference between heuristic labels and human judgments. Compared to counterfactual intervention, the CLEVRER heuristic is a closer approximation to human judgment. We think this is partially because we have kept the term “responsible for” used by CLEVRER other than “cause” in the human labelling interface. Fig. 2 provides two illustrative cases with explanations. We also provide detailed analysis on the effect of binarization thresholds and compositions of heuristics in the supplementary material.

3.2 Augment CLEVRER with Human Annotations

The key representation we will be using to augment CLEVRER is the Causal Event Graph (CEG), which has been adopted in similar datasets on video causal reasoning such as CRAFT [10] and video reasoning [36]. Each CEG $\mathcal{G} = (\mathcal{V}, \mathcal{E})$ is a graph structure of events and their causal relationships in a video. Each node $v \in \mathcal{V}$ is a natural language description of a physical event in the video, and each directed edge $(v_1, v_2) \in \mathcal{E}$ has a label in $\{positive, negative, unlabelled\}$ [‡]. A positive label for (v_1, v_2) denotes that event v_1 is a cause of event v_2 . CEGs directly enable downstream tasks such as physical and causal event generation, and causal relationship classification. Furthermore, based on the dense graph representation \mathcal{G} , we can generate questions about the causal relations, e.g., “Which event is responsible for the red cube moving?”

There are two desiderata for CEG annotations: diversity in event descriptions (nodes) and density in edge labels. Ideally, we want to ask human annotators to label all events in a video and relationships for all pairs of events. However, this is very time- and budget-consuming. Therefore, in practice, we use a three-stage annotation pipeline, as illustrated in Fig. 3. The first stage focuses on collecting human-written event descriptions using event cloze tasks, but only for a small number of videos. In the second stage, we augment the data for all videos using neural event description generators trained on the data collected from the first stage. In the third stage, we condense CEGs by collecting binary causal relation labels for all pairs of events from humans. All data are collected using the Mechanical Turk (MTurk) platform.

3.3 Stage I: Event Cloze

In the first stage, we use an event cloze task to collect human-written event descriptions. Cloze tests have been employed in various natural language processing (NLP) domains, such as narrative

[†]For simplicity, we use the word “cause” in this section. In the original CLEVRER dataset, such a relationship is formally defined as “A is responsible for B.”

[‡]Note that CEGs are generally different from causal graphical models because edges in CEGs are manually labelled and they reflect human judgement. Thus, they may not comply inference rules in graphical models.

Object State	Relative Position	Collision
Object A comes/moves/is hurled from some direction.	Object A is in the path of object B.	Object A is hit/struck by object B
Object A is thrown/pushed from some direction.	Object A is aimed at object B.	Object A hits/collides with/bumps into/runs into object B
Object A changes direction (towards some direction)	Object A moves together with object B	Object A is avoided hitting object B.
Object A stops moving		Object A pushes object B into object C.

Table 3: Event examples collected in the first stage, categorized into single-object states, pairwise relative positions, and pairwise collision events.

cloze [37], reading comprehension [38] and story-telling [39]. In contrast to these existing work, we develop a novel *iterative* data collection procedure as shown in Figure 4. For each video, we initialize its CEG with a single node using an event description from CLEVRER. Then we iteratively sample a node in the CEG, and ask humans to annotate a cause event or an effect event of the sampled event.

Specifically, the MTurk interface contains a single video and an incomplete sentence about two events in the video, connected by a “because” discourse marker: “___ because the yellow cylinder collides with the purple square.” In this case, the human-written event is an effect of the event specified in the sentence. Similarly, we use the template “Event A happens because ___.” to collect cause events. Most notably, the newly collected events will be used as the seeding event in the next iteration. This progressive design thus improves the diversity and coverage of the collected event descriptions.

In this stage, we select 100 videos from the CLEVRER training set with the largest number of collisions since we want to work with videos with especially rich causal relationships. In total, we obtain 1,724 event descriptions from 100 CLEVRER videos through crowdsourcing. We recognize three major types of events in the stage I dataset as shown in Table 3.

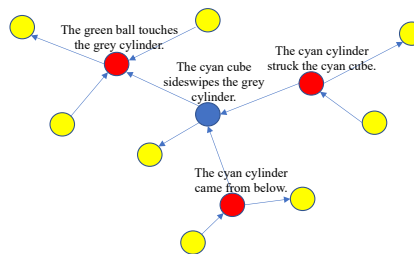


Figure 4: We use a novel iterative data collection procedure to collect CEGs on MTurk. Starting from a single node (iteration 0, blue), we iteratively sample nodes in the current CEG and collect either a cause or an effect event, and add this new node to the CEG. Red: nodes added in the first iteration; yellow: nodes added in the second iteration.

3.4 Stage II: Trajectory-based Event Description Generation

In the second stage, we leverage the manually written event descriptions to train neural description generators and augment the event description data for all videos. Our overall pipeline is shown in Fig. 5. Given the input video, it uses two branches to generate single-object events and pairwise events. The generated event descriptions will be sent to a post-processing module. It is important to note that the design choices in this stage focus on the *coverage* (i.e., we want to recover as many events from the input video as possible). All generated descriptions will be filtered again by MTurkers.

Trajectory representation. Instead of working with pixels, all event generation modules take symbolic representations of object trajectories as their inputs. Specifically, each video is represented by a set of trajectories $\{s_{i,t}\}$, where $s_{i,t}$ is the state of object i at timestep t . The state contains the color, shape, and material properties of object i , as well as its 3D position, velocity, and angular velocity at time step t . Since the CLEVRER videos are generated using simulated physical engines, this information can be directly obtained. Compared with images, trajectory-based inputs are lower-dimensional, and empirically yield significantly better results than pixel-based inputs when trained on a limited amount of data.

Data pre-processing. To associate human-written event descriptions with a single object or a pair of objects, we first run noun-phrase detection methods[§] on all descriptions. Next, we use all concept

[§]In particular, we used the tools from spaCy: <https://spacy.io/>.

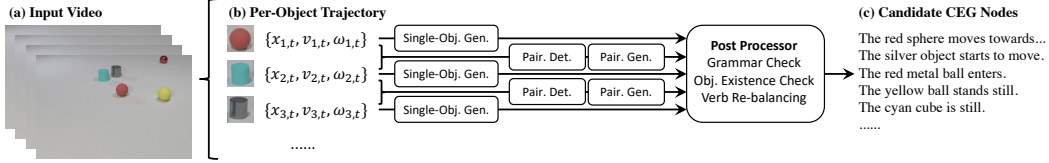


Figure 5: The neural event description generation pipeline (Stage II). (a) Given the input video, (b) we first extract per-object trajectories, composed of their attributes, positions, velocities, and angular velocities. For each object, we use a single-object event generator to sample event descriptions. For each pair of objects, we use a cascaded generator composed of a rule-based event detector and a neural pairwise generator. All generated events will pass a post-processing unit composed of three stages: grammar check, object existence check, and verb re-balancing. (c) The final product of the pipeline is a candidate node set of the CEG, which will be further annotated by humans in Stage III, the CEG condensation stage.

words in the detected noun phrases to filter the objects being referred to. The concept vocabulary contains colors, shapes, and materials, and is manually annotated. Based on the detected objects, we categorize each description into single-object (pairwise) events, and associate them with the corresponding object (pair of objects).

Single-Object event description. The single-object event generator is a GRU-based sequence-to-sequence model with attention [40]. It takes the trajectory of a single object throughout the video as input and generates natural language descriptions of events associated with this object. This module is trained on all of the 740 single-object descriptions from stage I.

Pairwise event description. Unlike single-object events, an important feature of pairwise events is *sparsity*. Specifically, for most pairs of objects in the video, there is no event associated with them. However, because we don’t have *negative* data in pairwise events (i.e., there are no descriptions such as “*object A and object B do not have interactions.*”), direct training of pairwise event generators will yield a lot of false-positive detection during test time.

To address this issue, we employ a rule-based object pair filter before the event generation process. Concretely, the event detector takes in the trajectories of a pair of objects and outputs whether an event occurs for the input pair. It first detects the longest consecutive (increasing/decreasing) sequence of object positions to segment the input trajectories. Then it processes each segment based on the physical properties in the trajectory. Based on manual inspection of stage-I data, we use rules to detect three types of events: object approaching, collision, and moving together. This is a simple but effective pre-processing step. By choosing the threshold, our detector has a recall rate of 99.2% on a small manually labeled dataset consisting of 100 videos. On the same split of 100 videos, the event detector improves the pairwise event description accuracy, labeled by human annotators in stage III, from 80.6% to 87.2%. For all pairs selected by the pairwise event detector, we concatenate their trajectories and feed them into a separate GRU-based sequence-to-sequence model. Similar to the single-object generator, this model is trained on all of the 984 pairwise descriptions from stage I.

Post-processing. We employ three post-processing steps to ensure the quality and diversity of generated event descriptions: grammar checking, object existence checking, and verb re-balancing. We first generate a large set of event descriptions (top-10 likely sequences per object and per pair). Next, we perform a grammar check using hand-crafted rules to filter common grammar errors such as missing verbs or missing verb arguments. Then, we detect noun phrases in the event descriptions and use concept words to select the object being referred to. We drop event descriptions that refer to objects that do not appear in the video. Finally, we notice that due to the sampling strategy, descriptions with the highest probabilities are not diverse: for example, for pairwise events, most highest-probability descriptions are about object collisions. Thus, we re-balance the data distribution based on the main verb of the descriptions. Specifically, we match this distribution with the human-written descriptions in stage I. For each video, we randomly sample at most 10 event descriptions.

3.5 Stage III: CEG Condensation

Finally, based on event descriptions generated in the second stage, we build dense CEGs using MTurk. In contrast to the first stage, where we use an event cloze task to collect natural language descriptions, in this stage, we focus solely on edge labeling: classifying whether two events have a causal relation.

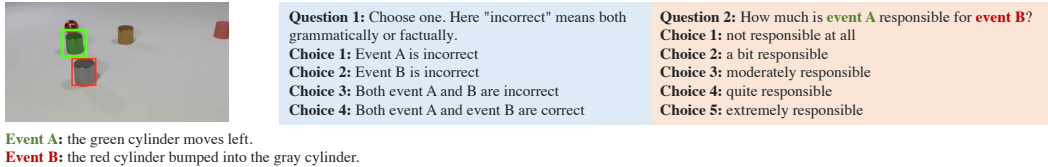


Figure 6: The MTurk interface illustration for the second stage. The MTurker sees the input video with objects mentioned in the events highlighted with colored bounding boxes. The MTurker answers two questions about the video: 1) whether event descriptions are correct and 2) a graded judgement of whether event A is responsible for event B. We use the same wording choice “be responsible for” to be consistent with the original CLEVRER dataset [7].

Concretely, we use an interface depicted in Fig. 6. The annotator is presented with a video, with objects being referred to in event descriptions highlighted in different colors. The annotator needs to answer two questions. The first question asks whether two event descriptions are interpretable (e.g., grammatically correct) and correct (i.e., they happen in the video). If the annotator labels both descriptions correct, they need to answer a second question, asking for a graded judgment (score 1-5) about whether the first event is a cause of the second event.

Based on the responses, we drop CEG nodes where a majority of the annotators label incorrect. The labeled edges have a score ranging from 1 to 5. We binarize the labels with a threshold of 4. That is, all edges with scores greater than or equal to 4 are considered positive.

3.6 QA conversion

To be compatible with the existing dataset CLEVRER, we further convert the CEGs to multiple-choice question-answer pairs. For every node v in the CEG \mathcal{G} with an adequate amount of positive parents (i.e. “causes”), we uniformly sample the number of correct choices in the question. We convert it to a question “Which of the following is responsible for A ?” and sample the set of positive and negative answers following the practice of CLEVRER. This ensures that the distribution of positive and negative candidates is balanced, as in the original CLEVRER dataset. We use the same train, validation, and test splits as CLEVRER.

3.7 Dataset Statistics

Overall, in CLEVRER-Humans, we retrieved 1108 videos with 8581 descriptions and 21167 event relationship annotations, after dropping empty CEGs. Based on the CEGs, we generate 1076 question-answer pairs. We will discuss the statistics of CLEVRER-Humans in detail in the supplementary material. In this section, we summarize four important features of CLEVRER-Humans.

First, CLEVRER-Humans contains dense annotations of causal relations between physical events. The average number of CEG nodes is 4.71, and the average number of labeled edges is 12.7. These dense annotations of CEGs form the rich and complicated causal structures in our dataset. Second, CLEVRER-Humans offers diverse free-form language descriptions while retaining balances in object properties. CLEVRER-Humans has a vocabulary length of size 219, which is much greater than CLEVRER (82). Next, most importantly, CLEVRER-Humans engage in a variety of physical events for causal reasoning tasks. In particular, CLEVRER-Humans contains 31 distinct verbs, and verbs are used in different tenses. In comparison, the original CLEVRER dataset contains only three event types (and verbs): enter, exit, and collide. Therefore, CLEVRER-Humans significantly improves diversity and brings in a challenge for machines to recognize and ground these events in practice. Finally, CLEVRER-Humans’ annotation reflects the subjective judgment of causality in physical events. CLEVRER-Humans offers 5 choices when asking MTurkers to label the causality level. The average score is 2.37. Note that this distribution is skewed towards lower scores. This reflects the fact that most event pairs do not have causal relationships. Finally, although we have binarized the edge labels for the sake of consistency with CLEVRER, the raw score-based judgment can be potentially helpful in other tasks, such as cognitive science studies.

Therefore, we can conclude that CLEVRER-Humans is a high-quality causal relation dataset with significantly more diverse event types and language descriptions than CLEVRER.

4 Experiments

In this section, we present the question-answering results of a collection of baseline methods on our new dataset CLEVRER-Humans. Since we have adapted the same input-output interface as the original CLEVRER dataset [7], most methods that are applicable to CLEVRER can also be applied to our dataset. In particular, we compare the following representative ones and highlight the challenge of our diverse and human-annotated physical and causal reasoning task.

4.1 Methods

Per-option best guess. The most basic baseline, per-option random guess (Guess) classifies each option with the most-frequent answer (“No” in our dataset).

Language-only models. We use language-only models to test potential language biases in the dataset. Specifically, we use an LSTM encoder [41] to encode the natural language question and the option, concatenate the last hidden state of both sequences, and apply a linear layer for binary classification.

Program-based video QA models. We also compare our model with NS-DR [7] and VRDP [42], two state-of-the-art video reasoning models based on program representations of questions. In particular, both methods leverage a semantic parser to parse questions and options into symbolic programs with hierarchical structures and execute the program based on the abstract video representation extracted by an object property network (NS-DR), or neuro-symbolic concept learning modules (VRDP). We train the semantic parser on the original CLEVRER dataset using the ground truth program annotations and use it to parse newly-annotated CLEVRER-Humans questions.

End-to-end video QA models. We also evaluate three additional end-to-end video QA models: CNN+LSTM, CNN+BERT, and ALOE [43]. In CNN+LSTM, we use CNNs to encode each frame into latent vectors and use two separate LSTMs to encode the video sequence and questions, respectively. The output of both video LSTM and the question LSTM are concatenated and fed into another linear layer to make binary classifications. The CNN+BERT model uses a similar architecture except that we replace the LSTM encoder with a pretrained BERT encoder [44]. ALOE [43] is the state-of-the-art video reasoning model on CLEVRER. It is based on the Transformer architecture [45]. It uses MoNET [46] to extract an object-centric representation of videos, uses a multi-modal transformer to encode both object features and questions, and predicts the binary label.

4.2 Results

Our results are summarized in Table 4. For both program-based models, since we do not have program annotations for CLEVRER-Humans questions and options, they are trained only on the original CLEVRER dataset and tested on CLEVRER-Humans. For both end-to-end models, we compare three alternatives: trained on CLEVRER, trained on CLEVRER-Humans, and pretrained on CLEVRER and then finetuned on CLEVRER-Humans. For most models that are pretrained, we used the checkpoints released by the authors. Thus, we are unable to compute confidence intervals.

Overall, all methods perform poorly on our dataset CLEVRER-Humans, especially when compared with the best guess model. In general, these results highlight three distinctive challenges of CLEVRER-Humans. First, the diversity of events: the vocabulary of CLEVRER-Humans questions and options are significantly richer than the original CLEVRER dataset. As a result, the performance of models pretrained on CLEVRER significantly drops (compared to their CLEVRER performances). In particular, the original CLEVRER dataset only has a vocabulary size of 82, while CLEVRER-Humans has a vocabulary size of 219. To directly apply pretrained models, we have to encode a large portion of textual inputs as “out-of-vocabulary.” Furthermore, by comparing CNN+LSTM and CNN+BERT, we see that using pretrained language models is not necessarily helpful for generalization to unseen events. The second challenge that accounts for the performance gap between the original CLEVRER and our dataset is human-annotated causal judgments: we do not see a significant difference between models trained from scratch on CLEVRER-Humans and the ones pretrained on CLEVRER in terms of the final performance, which empirically suggests the gap between causal relation labels between two datasets. A third challenge that arises from training-from-scratch or finetuning is the limited size of the CLEVRER-Humans training set. Recall that our dataset is directly comparable with the “explanatory questions” category of CLEVRER. CLEVRER contains 122,461 explanatory question pairs, while CLEVRER-Humans contains 1076 pairs. As a result, we

Model	Training	CLEVRER		CLEVRER-Humans	
		Per-Option	Per-Ques.	Per-Option	Per-Ques.
Best Guess	N/A	50.2	16.5	50.7	31.6
Lang-Only	Scratch	59.7	13.6	51.9 (\pm 1.09)	30.4 (\pm 1.90)
NS-DR [7]	Pretrain	87.6	79.6	51.0	32.0
VRDP [47]	Pretrain	96.3	91.9	50.9	31.6
CNN+LSTM	Pretrain	62.0	17.5	50.3	30.0
CNN+LSTM	Scratch	N/A [†]	N/A [†]	51.7 (\pm 0.64)	34.2 (\pm 1.69)
CNN+LSTM	Pretrain+Finetune	62.0	17.5	51.5 (\pm 2.35)	30.8 (\pm 0.69)
CNN+BERT	Pretrain	55.1	11.5	52.9	32.0
CNN+BERT	Scratch	N/A [†]	N/A [†]	52.0 (\pm 2.34)	30.2 (\pm 2.41)
CNN+BERT	Pretrain+Finetune	N/A [†]	N/A [†]	50.1 (\pm 0.68)	30.4 (\pm 3.09)
ALOE [43]	Pretrain	98.5	96.0	54.0	26.9
ALOE [43]	Scratch	N/A [†]	N/A [†]	51.8 (\pm 1.00)	31.7 (\pm 0.79)
ALOE [43]	Pretrain+Finetune	98.5	96.0	52.7 (\pm 1.36)	32.1 (\pm 1.36)
Human	N/A	N/A	N/A	84.5	71.4

Table 4: Test performance of different models on both the original CLEVRER dataset and our new CLEVRER-Humans dataset. The training column denotes the training schema for different models (in percentage, and the \pm sign shows the 95% confidence interval computed across 5 different runs). We compare both per-option accuracy and per-question accuracy, following the original paper [7]. Note that the number of options per question is ~ 4 for CLEVRER and 2 for CLEVRER-Humans. N/A marker[†]: models trained only on CLEVRER-Humans.

observe extreme training-set overfitting for large models such as ALOE. While as training goes on, the training accuracy keeps increasing to 70%, the per-option test accuracy plateaus at 53.7% at a very early stage. The combined challenge of diversity and data-efficient learning can be potentially addressed by enabling better transfer learning from large pre-trained multi-modal models such as CLIP [48], and better physics-informed models [49]. We also include human performance on the test set. Participants with full professional or higher proficiency in English are asked to evaluate the results on 50 videos from the test set. The participants also provide the percentage of descriptions that appear natural to them, which is 90.0% on average.

5 Conclusion

We have presented CLEVRER-Humans, the first video reasoning dataset of human-annotated physical event descriptions and their causal relations. CLEVRER-Humans introduces a unique and important challenge of combined physical scene understanding, natural language understanding, and causal reasoning. Due to its limited size, CLEVRER-Humans should be primarily used for zero-shot evaluation or few-shot training. Our preliminary results on question-answering illustrate the challenge of interpreting diverse human-written event descriptions, making human-like causal judgments, and data-efficient learning. To collect the dataset within a reasonable budget, we introduce two important techniques for dataset collection: iterative cloze-based annotation of event descriptions, and hybrid event description generation using neural sequence-to-sequence models. Both techniques can be applied to elicit data for any similar relation (such as “before” and “supports”). An exciting challenge will be extending these methods to naturalistic videos, complex events, and ambiguous relations.

Throughout the evaluations in this paper, we have been focusing on a binarized version of the causal reasoning task. However, it is important that computational models can make graded judgements as humans do. While existing literature has studied graded causal reasoning in text domains [50, 51] and static images [52], we believe an important direction is to build better models that perform graded causal reasoning in dynamic videos.

Acknowledgements. We also thank Keyi Hu for her contributions to the dataset. This work is partly supported by the Stanford Institute for Human-Centered AI (HAI), the Samsung Global Research Outreach (GRO) Program, ONR MURI N00014-22-1-2740, and Adobe, Amazon, Analog, Bosch, IBM, JPMC, Meta, and Salesforce.

References

- [1] Leonard Talmy. Force dynamics in language and cognition. *Cognitive science*, 12(1):49–100, 1988. 1, 3
- [2] Phillip Wolff. Representing causation. *Journal of experimental psychology: General*, 136(1):82, 2007. 1, 2, 3
- [3] Tobias Gerstenberg, Noah Goodman, David Lagnado, and Joshua Tenenbaum. Noisy newtons: Unifying process and dependency accounts of causal attribution. In *CogSci*, 2012. 1
- [4] Peter W Battaglia, Jessica B Hamrick, and Joshua B Tenenbaum. Simulation as an engine of physical scene understanding. *PNAS*, 110(45):18327–18332, 2013. 1
- [5] Tobias Gerstenberg and Joshua B Tenenbaum. Intuitive theories. *Oxford handbook of causal reasoning*, pages 515–548, 2017. 1
- [6] Ari Beller, Erin Bennett, and Tobias Gerstenberg. The language of causation. In *CogSci*, 2020. 1, 2
- [7] Kexin Yi, Chuang Gan, Yunzhu Li, Pushmeet Kohli, Jiajun Wu, Antonio Torralba, and Joshua B Tenenbaum. CLEVRER: Collision events for video representation and reasoning. In *ICLR*, 2020. 1, 2, 3, 4, 8, 9, 10, 15, 23
- [8] Rohit Girdhar and Deva Ramanan. Cater: A diagnostic dataset for compositional actions and temporal reasoning. In *ICLR*, 2019. 1, 3
- [9] Steven Sloman. *Causal models: How people think about the world and its alternatives*. Oxford University Press, 2005. 2, 3
- [10] Tayfun Ates, Muhammed Samil Atesoglu, Cagatay Yigit, Ilker Kesen, Mert Kobas, Erkut Erdem, Aykut Erdem, Tilbe Goksun, and Deniz Yuret. Craft: A benchmark for causal reasoning about forces and interactions. In *ACL*, 2022. 2, 3, 5
- [11] Tobias Gerstenberg. What would have happened? counterfactuals, hypotheticals, and causal judgments. *PsyArXiv*, 2022. 2
- [12] Justin Johnson, Bharath Hariharan, Laurens Van Der Maaten, Li Fei-Fei, C Lawrence Zitnick, and Ross Girshick. CLEVR: A diagnostic dataset for compositional language and elementary visual reasoning. In *CVPR*, 2017. 3
- [13] Makarand Tapaswi, Yukun Zhu, Rainer Stiefelhagen, Antonio Torralba, Raquel Urtasun, and Sanja Fidler. Movieqa: Understanding stories in movies through question-answering. In *CVPR*, 2016. 3, 4
- [14] Yunseok Jang, Yale Song, Youngjae Yu, Youngjin Kim, and Gunhee Kim. Tgif-qa: Toward spatio-temporal reasoning in visual question answering. In *CVPR*, 2017. 3, 4
- [15] Jie Lei, Licheng Yu, Tamara L Berg, and Mohit Bansal. Tvqa+: Spatio-temporal grounding for video question answering. In *ACL*, 2019. 3, 4
- [16] Madeleine Grunde-McLaughlin, Ranjay Krishna, and Maneesh Agrawala. Agqa: A benchmark for compositional spatio-temporal reasoning. In *CVPR*, 2021. 3, 4
- [17] Ronan Alexandre Riochet, Mario Ynocente Castro, Mathieu Bernard, Adam Lerer, Rob Fergus, Véronique Izard, and Emmanuel Dupoux. Intphys: A benchmark for visual intuitive physics reasoning. *T-PAMI*, 2021. 3
- [18] Jiajun Wu, Ilker Yildirim, Joseph J Lim, Bill Freeman, and Josh Tenenbaum. Galileo: Perceiving physical object properties by integrating a physics engine with deep learning. In *NeurIPS*, 2015. 3
- [19] Anton Bakhtin, Laurens van der Maaten, Justin Johnson, Laura Gustafson, and Ross Girshick. Phyre: A new benchmark for physical reasoning. In *NeurIPS*, 2019. 3
- [20] Fabien Baradel, Natalia Neverova, Julien Mille, Greg Mori, and Christian Wolf. Cophy: Counterfactual learning of physical dynamics. In *ICLR*, 2019. 3
- [21] Zhenfang Chen, Kexin Yi, Yunzhu Li, Mingyu Ding, Antonio Torralba, Joshua B. Tenenbaum, and Chuang Gan. Comphy: Compositional physical reasoning of objects and events from videos. In *ICLR*, 2022. 3
- [22] Nazneen Fatema Rajani, Rui Zhang, Yi Chern Tan, Stephan Zheng, Jeremy Weiss, Aadit Vyas, Abhijit Gupta, Caiming Xiong, Richard Socher, and Dragomir Radev. Esprit: explaining solutions to physical reasoning tasks. In *ACL*, 2020. 3
- [23] Sangeet S Khemlani, Aron K Barbey, and Philip N Johnson-Laird. Causal reasoning with mental models. *Frontiers in human neuroscience*, 8:849, 2014. 3
- [24] Eugenia Goldvarg and Philip N Johnson-Laird. Naive causality: A mental model theory of causal meaning and reasoning. *Cognitive science*, 25(4):565–610, 2001. 3
- [25] Steven Sloman, Aron K Barbey, and Jared M Hotaling. A causal model theory of the meaning of cause, enable, and prevent. *Cognitive Science*, 33(1):21–50, 2009. 3

- [26] Joseph Y Halpern and Judea Pearl. Causes and explanations: A structural-model approach. part i: Causes. *The British journal for the philosophy of science*, 2020. 3
- [27] Tobias Gerstenberg, Noah D Goodman, David A Lagnado, and Joshua B Tenenbaum. A counterfactual simulation model of causal judgments for physical events. *Psychological Review*, 128(5):936, 2021. 3
- [28] Phil Dowe. *Physical Causation*. Cambridge University Press, 2000. 3
- [29] Ranjay Krishna, Kenji Hata, Frederic Ren, Li Fei-Fei, and Juan Carlos Niebles. Dense-captioning events in videos. In *ICCV*, 2017. 4
- [30] Luwei Zhou, Yingbo Zhou, Jason J Corso, Richard Socher, and Caiming Xiong. End-to-end dense video captioning with masked transformer. In *CVPR*, 2018. 4
- [31] Huaishao Luo, Lei Ji, Botian Shi, Haoyang Huang, Nan Duan, Tianrui Li, Jason Li, Taroon Bharti, and Ming Zhou. Univl: A unified video and language pre-training model for multimodal understanding and generation. *arXiv:2002.06353*, 2020. 4
- [32] Chen Sun, Austin Myers, Carl Vondrick, Kevin Murphy, and Cordelia Schmid. Videobert: A joint model for video and language representation learning. In *ICCV*, 2019. 4
- [33] Subhashini Venugopalan, Huijuan Xu, Jeff Donahue, Marcus Rohrbach, Raymond Mooney, and Kate Saenko. Translating videos to natural language using deep recurrent neural networks. *NAACL-HLT*, 2015. 4
- [34] Jeffrey Donahue, Lisa Anne Hendricks, Sergio Guadarrama, Marcus Rohrbach, Subhashini Venugopalan, Kate Saenko, and Trevor Darrell. Long-term recurrent convolutional networks for visual recognition and description. In *CVPR*, 2015. 4
- [35] Li Yao, Atousa Torabi, Kyunghyun Cho, Nicolas Ballas, Christopher Pal, Hugo Larochelle, and Aaron Courville. Describing videos by exploiting temporal structure. In *ICCV*, 2015. 4
- [36] Chunpu Xu, Chengming Li, Ying Shen, Xiang Ao, Ruifeng Xu, and Min Yang. Imagine, reason and write: Visual storytelling with graph knowledge and relational reasoning. In *AAAI*, 2021. 5
- [37] Nathanael Chambers and Dan Jurafsky. Unsupervised learning of narrative event chains. In *ACL*, 2008. 6
- [38] Takeshi Onishi, Hai Wang, Mohit Bansal, Kevin Gimpel, and David McAllester. Who did what: A large-scale person-centered cloze dataset. In *EMNLP*, 2016. 6
- [39] Nasrin Mostafazadeh, Nathanael Chambers, Xiaodong He, Devi Parikh, Dhruv Batra, Lucy Vanderwende, Pushmeet Kohli, and James Allen. A corpus and cloze evaluation for deeper understanding of commonsense stories. In *NAACL-HLT*, 2016. 6
- [40] Kyunghyun Cho, Bart Van Merriënboer, Dzmitry Bahdanau, and Yoshua Bengio. On the properties of neural machine translation: Encoder-decoder approaches. In *NeurIPS-W*, 2014. 7
- [41] Sepp Hochreiter and Jürgen Schmidhuber. Long short-term memory. *Neural computation*, 9(8):1735–1780, 1997. 9, 18
- [42] Zhenfang Chen, Jiayuan Mao, Jiajun Wu, Kwan-Yee K Wong, Joshua B. Tenenbaum, and Chuang Gan. Grounding physical concepts of objects and events through dynamic visual reasoning. In *ICLR*, 2021. 9
- [43] David Ding, Felix Hill, Adam Santoro, and Matt Botvinick. Attention over learned object embeddings enables complex visual reasoning. In *NeurIPS*, 2021. 9, 10
- [44] Jacob Devlin, Ming-Wei Chang, Kenton Lee, and Kristina Toutanova. Bert: Pre-training of deep bidirectional transformers for language understanding. *arXiv preprint arXiv:1810.04805*, 2018. 9, 19
- [45] Ashish Vaswani, Noam Shazeer, Niki Parmar, Jakob Uszkoreit, Llion Jones, Aidan N Gomez, Łukasz Kaiser, and Illia Polosukhin. Attention is all you need. In *NeurIPS*, 2017. 9
- [46] Christopher P Burgess, Loic Matthey, Nicholas Watters, Rishabh Kabra, Irina Higgins, Matt Botvinick, and Alexander Lerchner. Monet: Unsupervised scene decomposition and representation. *arXiv:1901.11390*, 2019. 9
- [47] Mingyu Ding, Zhenfang Chen, Tao Du, Ping Luo, Josh Tenenbaum, and Chuang Gan. Dynamic visual reasoning by learning differentiable physics models from video and language. In *NeurIPS*, 2021. 10
- [48] Alec Radford, Jong Wook Kim, Chris Hallacy, Aditya Ramesh, Gabriel Goh, Sandhini Agarwal, Girish Sastry, Amanda Askell, Pamela Mishkin, Jack Clark, et al. Learning transferable visual models from natural language supervision. In *ICML*. PMLR, 2021. 10
- [49] Jiajun Wu, Erika Lu, Pushmeet Kohli, Bill Freeman, and Josh Tenenbaum. Learning to see physics via visual de-animation. In *NeurIPS*, volume 30, 2017. 10
- [50] Melissa Roemmele, Cosmin Adrian Bejan, and Andrew S Gordon. Choice of plausible alternatives: An evaluation of commonsense causal reasoning. In *AAAI spring symposium: logical formalizations of commonsense reasoning*, 2011. 10

- [51] Sheng Zhang, Rachel Rudinger, Kevin Duh, and Benjamin Van Durme. Ordinal common-sense inference. *TACL*, 5:379–395, 2017. 10
- [52] Jinyoung Yeo, Gyeongbok Lee, Gengyu Wang, Seungtaek Choi, Hyunsouk Cho, Reinald Kim Ampayo, and Seung-won Hwang. Visual choice of plausible alternatives: An evaluation of image-based commonsense causal reasoning. In *LREC*, 2018. 10
- [53] Kyunghyun Cho, Bart Van Merriënboer, Dzmitry Bahdanau, and Yoshua Bengio. On the properties of neural machine translation: Encoder-decoder approaches. *arXiv:1409.1259*, 2014. 18
- [54] Jeffrey Pennington, Richard Socher, and Christopher D Manning. Glove: Global vectors for word representation. In *EMNLP*, 2014. 18
- [55] Diederik P Kingma and Jimmy Ba. Adam: A method for stochastic optimization. In *ICLR*, 2015. 18, 19
- [56] Kaiming He, Xiangyu Zhang, Shaoqing Ren, and Jian Sun. Deep residual learning for image recognition. In *CVPR*, 2016. 18
- [57] David Ding, Felix Hill, Adam Santoro, Malcolm Reynolds, and Matt Botvinick. Attention over learned object embeddings enables complex visual reasoning. https://github.com/deepmind/deepmind-research/tree/a5522d078413e340a2caalab0c86d76d2b7efa40/object_attention_for_reasoning, 2021. 19
- [58] Emily M. Bender and Batya Friedman. Data Statements for Natural Language Processing: Toward Mitigating System Bias and Enabling Better Science. *TACL*, 6:587–604, 12 2018. 23
- [59] Joel Ross, Lilly Irani, M. Six Silberman, Andrew Zaldivar, and Bill Tomlinson. Who are the crowdworkers? shifting demographics in mechanical turk. In *CHI Extended Abstracts on Human Factors in Computing Systems*, 2010. 23

Supplementary Material for CLEVRER-Humans: Describing Physical and Causal Events the Human Way

We bear all responsibility in case of violation of rights. The data created or used during this study are openly available on the project’s website (<https://sites.google.com/stanford.edu/clevrer-humans>). We confirm that the data is under a CC0 license. We will provide maintenance to the website and dataset regularly and upon request.

The rest of this supplementary document is organized as the following. First, in Section A we provide visualizations of data collected in CLEVRER-Humans, as well as more analysis on the comparison between human causal judgments and heuristics-based labels. In Section B, we describe the implementation details of models studied in the main paper and add additional failure case analysis of models. Next, in Section C, we describe the user interface for dataset collection. Finally, in Section D, we supplement dataset sheets for CLEVRER-Humans.

A Dataset Visualization and Analysis

Fig. 8 and Fig. 9 show the example graph collected in the stage I (causal event cloze) and stage II (binary CEG labelling), respectively. First, Fig. 8 shows that the causal cloze tasks can progressively collect a large number of human-written event descriptions by re-using the response of previous annotators. On average, we can obtain 29.4 descriptions per video, highlighting the advantage of our design. Second, the condensed CEGs contain high-quality causal relations of physical events, as shown in Fig. 9. It demonstrates both the language diversity and the richness of causal relations in the CEGs of CLEVRER-Humans. These figures provide a straightforward illustration of our data collection pipeline and the quality of our data.

A.1 Dataset Statistics

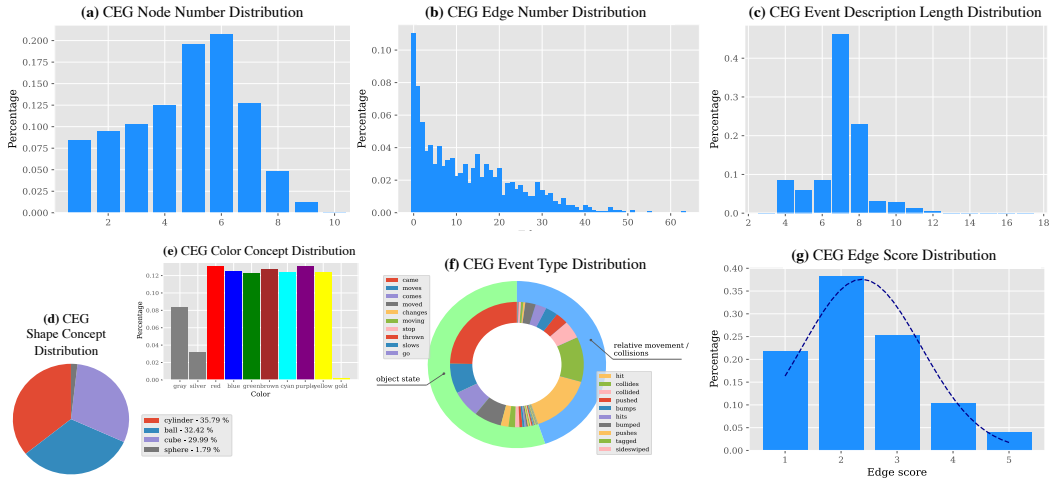


Figure 7: Statistics on the CLEVRER-Humans dataset. From left to right, the first row figures are distributions of (a) the number of nodes per CEG, (b) the number of edges per CEG, and (c) sentence lengths excluding the "which of the following is responsible for" prefix. The second row figures are distributions of (d) object shapes, (e) colors, (f) event type attributions based on verbs, and (g) CEG edge scores labelled by MTurkers, respectively.

First, CLEVRER-Humans contains dense annotations of causal relations between physical events. Fig. 7a and Fig. 7b show the distributions of the number of nodes and edges in each CEG. The average number of CEG nodes is 4.71, and the average number of labeled edges is 12.7. These dense annotations of CEGs form the rich and complicated causal structures in our dataset.

Second, CLEVRER-Humans offers diverse free-form language descriptions while retaining balances in object properties. Fig. 7c shows the length distribution of event descriptions: the average length is 7.00 (as a reference, the average event description length of CLEVRER is 8.93). CLEVRER-Humans

	$Y = y_1$	$Y = y_2$	$Y = y_1 \wedge y_2$	$Y = y_1 \vee y_2$	$Y = y_1 \oplus y_2$
$P(X = \text{Human} \mid Y)$	0.62	0.61	0.23	0.34	0.34
$P(Y \mid X = \text{Human})$	0.96	0.54	0.29	0.62	0.33

Table 5: Comparison between different combinations of heuristics-generated causal labels and human labels, on a sampled subset of CLEVRER [7]. The entry $P(X|Y)$ denotes the fraction of event relations that are annotated as causal by protocol X given that the relations are annotated as causal by protocol Y. y_1, y_2 denote the existence of causal relations defined CLEVRER’s heuristic and Counterfactual causal relation, respectively.

has a vocabulary length of size 219, which is much greater than CLEVRER (82). Fig. 7d and Fig. 7e show the distribution of object property concepts: colors and shapes. They remain unbiased when considering the synonyms such as “ball” and “sphere” and “gray” and “silver.”

Next, most importantly, CLEVRER-Humans engage in a variety of physical events for causal reasoning tasks. In particular, Fig. 7f shows the distribution of event types computed based on the main verb of the event description. The outer circle represents the general event families. The corresponding inner breakdowns display more than 10 variations of the expression based on verbs for each event type. In comparison, the original CLEVRER dataset contains only three event types (and verbs): enter, exit, and collide. Therefore, CLEVRER-Humans significantly improves diversity and brings in a challenge for machines to recognize and ground these events in practice.

In the following box, we list all verbs that have been annotated by human annotators and generated by our machine generative model. We have lemmatized all verbs to remove the tense.

come, move, change, stop, throw, slow, go, travel, begin, spin, roll, stand, halt, roll, lose, leave, head, want, hurl, enter, hit, collide, push, bump, push, tag, sideswipe, bounce, strike, touch, cause

We also would like to point out that for some verbs, if they seem to be synonyms (e.g., bump and sideswipe), they can have subtle differences in physical grounding. For example, A bumping into B usually implies that A is moving faster than B and its collision changed the state of B. Furthermore, the different tenses of the same verb have different meanings in sentences: "the event that ball A moved is responsible for the collision" is different from "the event that ball A is moving is responsible for the collision." In the former case, ball A does not have to be moving while the collision happens.

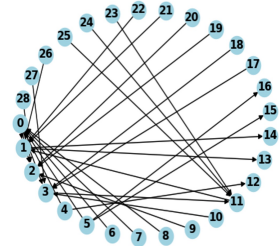
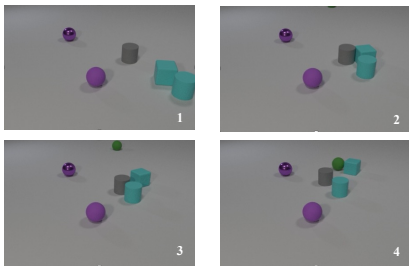
It is possible to hand-craft a lot of rules to handle each individual case (e.g., bump, sideswipe, roll), but that will require additional hyperparameters for thresholds, and may be hard to align with human perception.

Finally, CLEVRER-Humans’ annotation reflects the subjective judgment of causality in physical events. CLEVRER-Humans offers 5 choices when asking MTurkers to label the causality level. Fig. 7g shows the distribution of edge scores with an average of 2.37. Note that this distribution is skewed towards lower scores (as shown by the Gaussian approximation in the dotted curve). This reflects the fact that most event pairs do not have causal relationships. Finally, although we have binarized the edge labels for the sake of consistency with CLEVRER, the raw score-based judgment can be potentially helpful in other tasks, such as cognitive science studies.

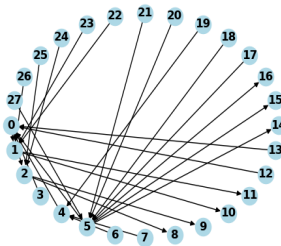
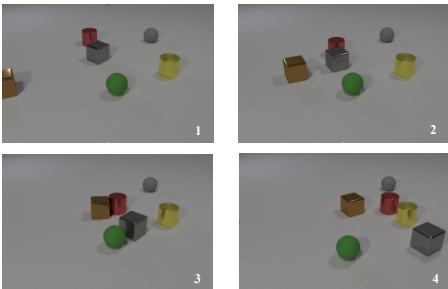
Therefore, we can conclude that CLEVRER-Humans is a high-quality causal relation dataset with significantly more diverse event types and language descriptions than CLEVRER.

A.2 Comparison between Heuristic and Human Causal Judgments

We supplement the effect of different thresholds on the graded causal relation in Fig. 10. In the human performance study, we asked the participants to choose a threshold from 1-5 if they had to binarize their judgment. The average threshold suggested by the participants is 3.6. In practice, we choose a threshold of 4 to obtain the causal relation that humans are more certain about.



- 0: the cyan cube sideswipes the grey cylinder
- 1: the green ball hits the cyan cube
- 2: the green ball touches the grey cylinder
- 3: the green ball bumps into the cyan cube
- 4: the cyan cube was moving in direction opposite to the grey cylinder
- 5: the cyan cylinder came from below
- 6: the cyan cylinder struck the cyan cube
- 7: the cyan cube was struck by the cyan cylinder
- 8: the cyan cylinder moved
- 9: the green ball was pushed by the cyan cube
- 10: the gray cylinder moved
- 11: the green ball came from above
- 12: the square cyan was hit by the cyan cube causing the grey cylinder to move away
- 13: the cyan cube is pushed to the right side
- 14: the cyan cube spins counterclockwise
- 15: the green ball collided with the cyan cube
- 16: grey cylinder moved forward
- 17: the blue rubber cylinder bumped the cyan cube in the way of the green ball
- 18: the green ball slides down into the scene into the cyan cube
- 19: the green ball touched the cyan cube
- 20: the green ball bounces off the cyan cube and touches the grey cylinder
- 21: cyan is on a direct path to green ball path
- 22: the cyan cylinder hits the cyan cube
- 23: the green ball was already moving downwards
- 24: the green ball had velocity
- 25: the green ball rolled down into the screen and bounced into the cyan cube
- 26: the cyan cylinder hit the cyan cube
- 27: the green ball and the cyan cube were heading to the same point
- 28: the green ball bounces off the blue square which was traveling in the opposite direction



- 0: the brown cube starts to spin clockwise
- 1: the brown cube hits the silver cube and then hit the red cube
- 2: the brown cube came from the west
- 3: the brown cube starts to spin clockwise because gold metal shere to swipe
- 4: the brown cube hits the metal purple cube
- 5: the brown cube hit the ash cube by the side
- 6: the metal purple cube was in the way
- 7: the red cylinder collides with the metal purple cube
- 8: the grey cube touched the green ball
- 9: the grey cube moved south
- 10: the red cube ends up in the east
- 11: the silver cube hits the green ball
- 12: the brown cube collided with the silver cube after the silver cube was struck by the red cylinder
- 13: the brown cube collided with the grey cube
- 14: the ash cube moves to the right
- 15: the gray cube spun
- 16: the silver cube hit the green ball
- 17: the red cylinder collided with the yellow cylinder
- 18: the red cylinder pushed the ash cube away from the brown cube's path
- 19: the red cylinder hit the metal purple cube
- 20: the brown cube came from the left
- 21: the red cylinder hit the ash cube from the top
- 22: ricochets off to left and bounces into red cube
- 23: the brown cube came from the side
- 24: the brown cube started off on the west and was moving east
- 25: the brown cube was pushed by an unknown and unseen force
- 26: the silver cube absorbed the force from the brown cube in order to hit the red cube
- 27: the red cylinder hit the grey cylinder which changed its direction

Figure 8: Visualization of two samples of annotations collected in Stage I causal cloze tasks. They are collected progressively by feeding the response of a user as the input of another one. The black arrows indicate the annotation orders.

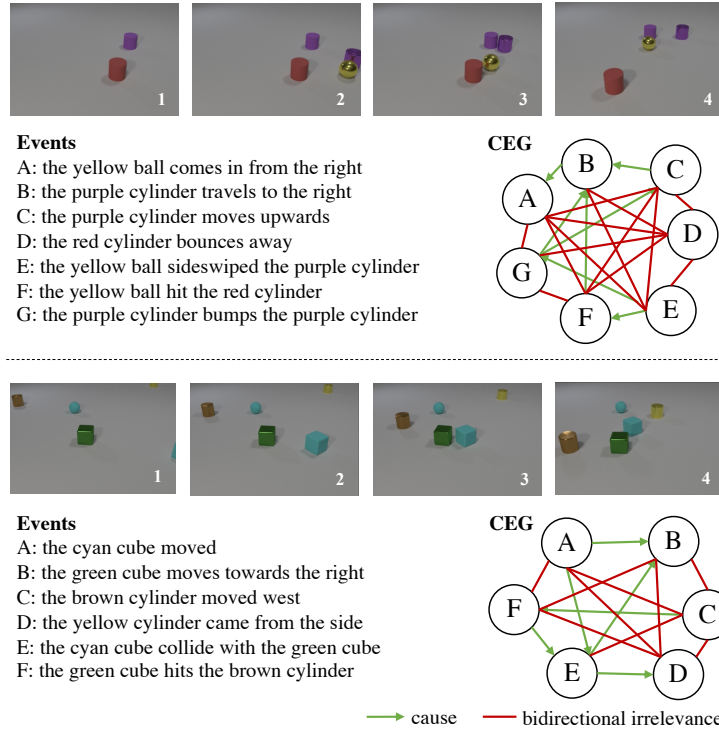


Figure 9: Visualization of two samples of CEGs in CLEVRER-Humans. The green arrows represent causal relations and the red edges represent bidirectional irrelevance. We can see the rich causal relations among physical events presented in the CEGs.

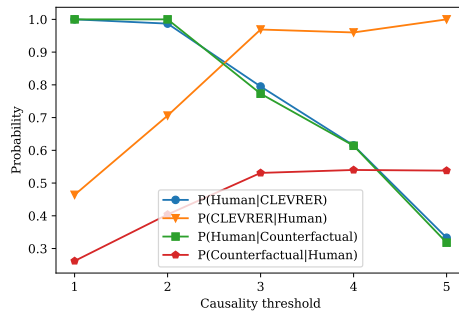


Figure 10: Effect of different causality thresholds on the binarized human causal relation. The x-axis is the ablation threshold (i.e., 4 means a score ≥ 4 represents a causal relation). The y-axis is the conditional probability.

Having shown the two common heuristics-generated causal labels (CLEVRER’s and counterfactual intervention) diverge from human judgment, we also provide the results on comparisons between different combinations of heuristics-generated causal labels and human judgments. We use the logic operators and (\wedge), or (\vee), xor (\oplus). As shown in Table 5, none of these combinations can give a close enough approximation to human judgment, which further justifies our motivation to use human-labeled causal data for CLEVRER-Humans.

B Implementation Details

In this section, we present the implementation details of our neural network-based event description generator, the baseline models studied in the main paper, and the error bars for models across different random seeds.

B.1 Stage II Implementation

We first describe the input pre-processing for neural event generators. For each object, we concatenate the one-hot encoding of physical properties (including shapes, colors, and materials) and the motion information (including location, orientation, velocity, angular velocity, and whether the object is inside the camera view) in each of the 128 frames in a video. For each object, at each time step, the input dimension is 24.

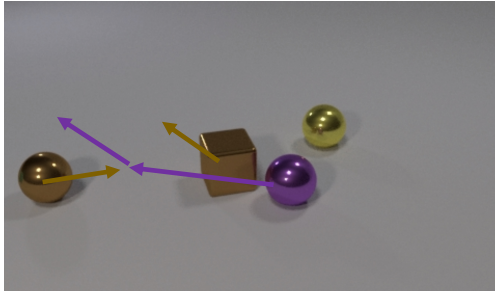
Our rule-based event detector for object pairs works as the following. For object pairs, we first extract all segments that are composed of consecutive frames when two objects are close to each other. Specifically, we say two objects are close if the L_∞ norm of the displacement vector between two objects is smaller than 0.5 meters (i.e., their x, y, z displacements are all smaller than 0.5 meters). Within each segment, the event detector predicts event types, including moving together, object approaching, and collision, based on changes in the motion information. For example, if two objects are physically close for more than 20 frames without rapid changes in velocity, we consider them relatively static, thus “moving together.” If both objects change directions within their close period, we consider a collision happened. We can further distinguish the changes in relative positions (either “bouncing back” or “one approaching another”) by the sign of the dot product of velocity vectors. For any object pair, if no events are detected in the course of the entire video, we do not include this pair for future captioning.

After getting the input sequences, we use neural event generators consisting of an encoder and a decoder to produce captions. The encoder uses a linear layer and a GRU unit to encode the input sequence [53]. The decoder applies Softmax on the embedding of the input and the hidden state to produce the attention weights. It then uses GRU and a linear layer to produce an English caption of specific objects in the video. Single-object and pairwise captioning models share the same architecture but are trained independently. The hidden dimension of both the encoder and the decoder is 256 for single-object models and 128 for pairwise models. The dropout rate for the decoder is set to 0.3 for single-object models and 0.1 for pairwise models. All models are trained with a learning rate of 0.001. For the grammar check module in the post-processor, we drop the sentences with two consecutively repeated words. We also exclude the sentences that miss verbs or verb arguments, such as sentences ending with words “from,” “to,” “at,” “is,” etc.

B.2 Baseline Implementation

Language-Only models. For the language-only models, we use a LSTM [41] with GloVe [54] word embedding. The hidden dimension is 512, and the dropout rate is 0.2. We use the Adam optimizer [55] with a learning rate is 4×10^{-4} and a weight decay of 10^{-5} . The batch size is 4. Following the data splits in CLEVRER, we split 20% of the training pairs as the validation set and choose the model with the highest validation accuracy.

CNN+LSTM. For the CNN+LSTM models, we use a pre-trained ResNet-50 to extract 2,048-dimensional features from the video frames [56]. We uniformly sample 25 frames for each video as input. The word embedding for questions is initialized by the GloVe [54] word embedding. Both LSTMs (the question encoder and the video sequence encoder) have 1 layer with a hidden dimension of 512. We apply a dropout rate of 0.2 on the input layer and 0.5 on the hidden layers. We use the

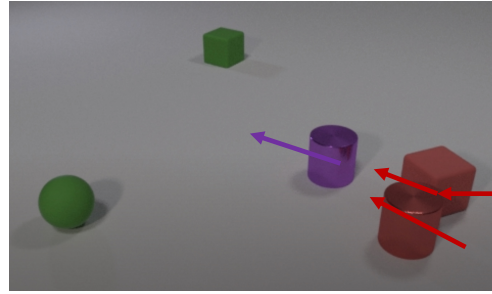


Question: What is responsible the purple ball collides with the brown cube?

Choice: The purple ball comes up.

Answer: Wrong

Model prediction: Correct



Question: What is responsible for the red cube sideswiped the purple cylinder?

Choice: The red cube bumped the red cylinder.

Answer: Wrong

Model prediction: Correct

Figure 11: Examples of common prediction errors. The arrows in the image represent the moving direction of objects of interest in the video. **Left:** failure caused by nuances in human language. While the purple ball is constantly moving upwards coordinate-wise, humans understand the phrase "comes up" as more of the later part of the trajectory (after the purple ball collides with the brown ball). Therefore, machines cannot give a correct prediction. **Right:** failure in bridging the domain shift. Humans may consider the change in the trajectory to be minor and appears not to be a deciding factor of the outcome event, but the model predicts it as a cause following similar heuristics in CLEVRER.

Adam [55] optimizer with a weight decay of 5×10^{-4} . The learning rate is 10^{-5} for training from scratch and 10^{-3} for finetuning. The batch size is 128 for both trained-from-scratch and finetuning experiments. We split 20% of the training pairs as the validation set and choose the model with the highest validation accuracy.

BERT+LSTM We supplement CNN+BERT models as a model with a stronger text encoder. The CNN is the same as in the CNN+LSTM baseline. We use the pretrained BERT uncased base model from HuggingFace library [44]. The BERT tokenizer is set to max length 32 padding and truncation. During training, We fix the weights of the text encoder. We use the Adam optimizer with a weight decay of 5×10^{-4} , and a learning rate of 10^{-5} training from scratch and 10^{-3} for finetuning. The batch size is 128. We choose the model with the highest validation accuracy with 20% of the training set as the validation set.

ALOE. We implement our model based on the publicly released code [57]. Since the public release does not contain training code, we implement the training procedure using the following settings. For object embeddings, we use the pre-trained MONet embeddings released by the authors. For optimization, we use the Adam [55] optimizer with a weight decay of 10^{-3} (we have also benchmarked 10^{-2} , 10^{-3} and 10^{-4}). We split 5% of the training pairs as the validation set and choose the model with the highest validation accuracy.

B.3 Error analysis

We summarize the common failures of the models: for pretrained-only models, the common error comes from the failure to incorporate more diverse language and events. For example, as shown in Table 6, the program parser of NS-DR and VRDP fails to generate proper programs for descriptions in CLEVRER-Humans. The deficiency of language understanding often leads to wrong predictions.

For training from scratch models, one possible reason for the test errors is the nuances in human language. Specifically, models do not only need to identify the objects being referred to but also their physical properties: the cause of "the red cube slows down" can be hard to identify because speed does not appear to be as explicit as other properties, such as colors and shapes. As shown in our comparison between human judgement and heuristics-based causal judgements, the nuance in language can influence human judgements, posing difficulties for machines to ground the events

Event	Parsed program
The purple sphere slows down from the right.	["events", "objects", "purple", "filter_color", "sphere", "filter_shape", "unique", "filter_collision", "objects", "unique", "filter_color", "sphere", "filter_shape", "unique", "filter_collision", "unique"]
The red ball comes to a stop.	["events", "objects", "red", "filter_color", "unique", "filter_collision", "objects", "red", "filter_color", "unique", "filter_collision", "unique"]
The yellow cube comes from the right side at a fast speed.	["events", "objects", "yellow", "filter_color", "cube", "filter_shape", "unique", "filter_out", "unique"]

Table 6: Examples of errors produced by program parser. In the first row, the model cannot identify the event "slow down from the right" and gives incorrect parsing to find another object involved in a collision ("filter_collision"). In the second row, the model cannot represent the event "come to a stop" due to the expansion in vocabulary and gives an incorrect output ("filter_collision"). In the third row, the model mistakenly represents the enter event as the exit event ("filter_out") because the description is more complicated in CLEVRER-Humans. We follow the notation of programs as in NSDR and VRDP.

and simulate the reasoning process. For instance, the left figure in Fig. 11 illustrates the nuances in language resulting in a discrepancy between human judgment and prediction. Moreover, for large models such as ALOE, learning to simulate human reasoning processes from scratch based on very little data can be difficult, especially with a limited training size.

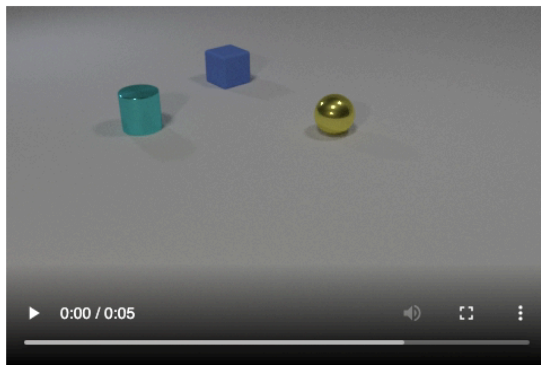
For finetuned models, we have not seen significant improvement brought by the pretraining phase. This is primarily because of the domain gap between human judgement and heuristics-based labeling. Specifically, our human experiments have shown that $p(\text{Human} \mid \text{CLEVRER-Heuristic}) = 0.62$. That is, only 62% of the event pairs that have been labeled as causal in CLEVRER, are labeled as causal by human annotators. The right figure in Fig. 11 gives an example of the error caused by the domain shift. Future work may consider other ways of pretraining, such as pretraining on event recognition, which may be more transferable, and pretraining with other types of heuristics.

C Labeling Interface

We develop labeling interfaces based on boto3 with Amazon MTurk python API. We include example trials of both the causal cloze tasks and CEG annotation tasks in Fig. 12 and Fig. 13, respectively. The full instruction texts are provided on the labeling page of our project’s website. The estimated hourly pay to the Mechanical Turk participants is about \$6.1, and the total amount spent on participant compensation is about \$3500. Specifically, the cloze tests and part of the pairwise causal relationship annotations were completed by users from the U.S., and the pay was \$7.7/hour (above the federal minimum wage). At a later stage of our project, we were unfortunately constrained by the budget available to us and opened the tasks to workers outside the U.S. Thus, overall, our average hourly wage is \$6.1. Our goal has always been to commit to best practices and offer fair pay to users whenever possible, and we will continue to do so in the future.

In causal cloze tasks, the participants are asked to write an event description given a cause or outcome event, as shown in Fig. 12. We specify the expectation of responses (such as using complete sentences, avoiding ambiguous third-person pronouns, etc.) in the instruction. We design a small comprehension quiz with 7 multiple-choice questions and 2 chances to submit to ensure the participants understand the instructions correctly.

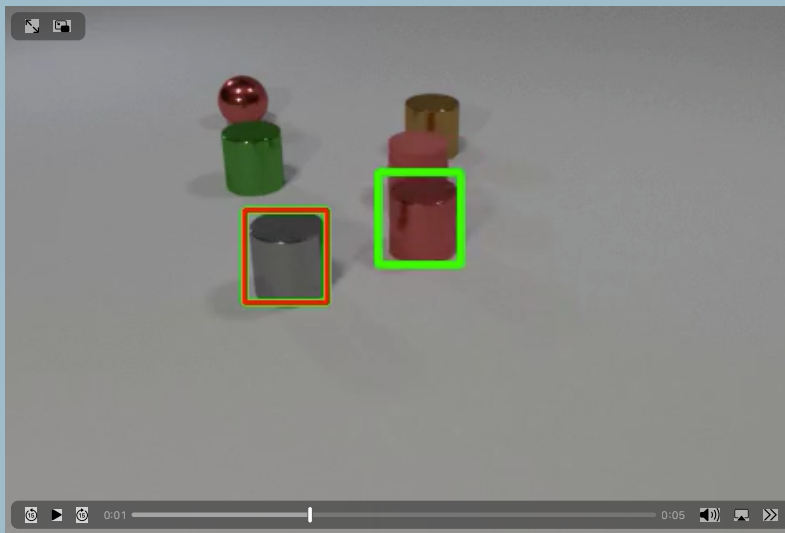
In the CEG annotation tasks, the participants are asked to label the correctness and causal relation of two event descriptions as shown in Fig. 13. We give 4 examples with detailed explanations to help them understand the rationale of the task. We also give an illustration of object colors and shapes for reference. Bounding boxes are added to the videos to accelerate the process of locating objects of interest.



because
the yellow cylinder collides with the purple square first.

- The prompt has no problem.
- I don't know what the prompt is talking about.
- The prompt makes sense to me but I cannot think of a way to fill in the blank.

Figure 12: Example of a causal cloze trial. The participants are asked to fill in the blank after watching a video. They can also select the checkboxes if they do not understand the prompt.



Event A: the red cylinder slides into the grey cylinder.

Event B: the grey cylinder moves left.

Question 1: Choose one. Here "incorrect" means either grammatically or factually.

- Event A is incorrect
- Event B is incorrect
- Both event A and B are incorrect
- Both event A and B are correct

Explanation: Choice 4 is selected because both event A and B are grammatically correct and they actually happened in the video.

Question 2: How much is **event A** responsible for **event B**?

- 1 - not responsible at all
- 2 - a bit responsible
- 3 - moderately responsible
- 4 - quite responsible
- 5 - extremely responsible

Explanation: One may think event A is highly responsible for event B as event A is the direct cause of event B. However, there's no right answer to this question - just select the answer you think is most reasonable.

Figure 13: Example of a CEG trial. The participants are first asked to select if the event descriptions are correct. If both correct, they are asked to label the level of causal relations between the descriptions. For each event pair, we provide bounding boxes for objects involved in the events for better annotation efficiency.

D Dataset Release

Our dataset is under CC0 License. We provide a documentation using data statements for NLP in [58].

Short form data statement CLEVRER-Humans is a large-scale video reasoning dataset of human-annotated physical event descriptions and their causal relations. It contains machine-generated texts based on crowdsourcing data in US English (en-US). The language quality and causal structure annotations are obtained by watching videos, reading texts, and entering responses on MTurk.

The following is the long-form data statement of CLEVRER-Humans:

Curation Nationale CLEVRER-Humans contains descriptions and causal relations of physical events such as an object entering the scene and two objects colliding with each other. The goals in selecting texts were to ensure the interpretability and correctness of the descriptions and to provide a variety of free-form captioning of physical events in videos. We first collected human-written event descriptions by causal cloze tasks, then used machine learning models to generate more natural language descriptions based on the curated data. We post-processed the data by grammar checking, object existence checking, and verb re-balancing. Finally, we obtained human annotations on the texts through crowdsourcing: if the labelers annotated the texts as interpretable and correct, we asked them to provide a pairwise graded causal judgment of the events.

Language Variety The event description data for causal cloze tasks were collected on MTurk. Information about which varieties of English are represented is not available, but at least CLEVRER-Humans includes US (en-US) mainstream English.

Speaker Demographic We used a cascaded generator composed of a rule-based event detector and a neural pairwise generator to generate texts. When curating training data in causal cloze tasks, we restricted the location of these MTurkers to be in the US. It is expected that most speakers use English as their native language. Estimated demographics of MTurkers may refer to [59].

Annotator Demographic We hire MTurkers with approved HITs of 1000 or higher. We expect the MTurkers to be the general public who are familiar with the basic crowdsourcing process. When collecting data, we release the tasks in batches, where each HIT contains 30 QA pairs, mostly coming from one or two videos. We perform a quality check to ensure annotators have sufficient knowledge of the English language. We also answer their questions about the annotation process by email. It is expected that most speakers use English as their native language. Estimated demographics of annotators may refer to [59].

Speech Situation The intended audience of the texts is the general public. The texts are all in written form. MTurkers are expected to read the text and watch the video when doing causal cloze and causal labeling tasks. The video is about 5 seconds, which can be played as many times as one wishes.

Text Characteristics The texts are plain English descriptions of a physical event in a video. A sentence usually contains one or more physical object(s) (i.e. sphere, cylinder, or cube) and the related movements or interactions presented in the video. Ideally, the generated event descriptions can maintain the vocabulary and structural characteristics similar to the training data from causal cloze tasks. The detailed statistics of the text are shown in the Dataset Statistics section.

Recording Quality N/A

Other N/A

Provenance Appendix The videos of CLEVRER-Humans are from the CLEVRER dataset [7].

D.1 Intended Use

CLEVRER-Humans can be used as a benchmark in physical scene understanding and causal reasoning. It evaluates machines' ability to understand and analyze physical interventions in a restricted setting. Machines are provided with a short video and expected to answer questions regarding the causes of events in the video.

D.2 Maintenance Plan

We will host our dataset permanently on our project's website. Users are granted access to the dataset through links on the website. We provide versioning of the dataset and archive backup regularly.

D.3 Quality Check

Quality checks over CEG node correctness are performed by majority voting. Since we have allocated the annotation of each video to 3 annotators, and they will see overlapping events and annotate their correctness. Checks for edge correctness are performed by including additional "quality checking" questions. Specifically, each annotator will see 3 videos and 10 questions for each video. 1 of the video will be from a small and manually-curated dataset by authors, containing 30 videos. The entire answer set will be accepted if and only if the annotators answer those quality-checking questions correctly (more specifically, have a small divergence from our answer).